Smooth composite pulses for high-fidelity quantum information processing

Boyan T. Torosov and Nikolay V. Vitanov

Phys. Rev. A **83**, 053420 — Published 23 May 2011

DOI: 10.1103/PhysRevA.83.053420

Smooth composite pulses for high-fidelity quantum information processing

Boyan T. Torosov and Nikolay V. Vitanov
Department of Physics, Sofia University, 5 James Bourchier blvd, 1164 Sofia, Bulgaria

We present a systematic SU(2) approach for construction of composite sequences of pulses with *smooth* temporal shapes that produce high-fidelity two-state excitation profiles. This makes possible the application of composite pulses to quantum control and quantum information processing with short and ultrashort laser pulses. We present an exact analytic formula for the composite phases for arbitrarily accurate broadband pulses, examples of narrowband, passband and fractional-π pulses, as well as composite pulses with detuning compensation.

PACS numbers: 32.80.Qk, 42.65.Re, 82.56.Jn, 42.50.Dv

I. INTRODUCTION

The technique of composite pulses developed originally in nuclear magnetic resonance (NMR) [1–9] is a powerful tool for quantum state manipulation. This technique replaces the single pulse used traditionally for driving a two-state transition in a quantum system by a sequence of pulses with appropriately chosen phases, which are used as a control tool for shaping the excitation profile in a desired manner. In particular, a nearly perfect population inversion, which is insensitive to variations in the interaction parameters — the amplitude and/or the frequency of the pulses — can be achieved. This technique therefore combines the accuracy of single π-pulse excitation with a robustness similar to adiabatic techniques. For this reason, composite pulses have enjoyed steadily increasing attention in the field of quantum computation, wherein ultrahigh fidelity of gate operations is required, e.g., in implementation of quantum gates and quantum algorithms with trapped ions [10–15].

The existing methods for design of composite pulses are developed for pulses of rectangular temporal shape, which is suited for NMR experiments [1–9], as well as for atomic excitation with microsecond pulses [10–15]. However, rectangular pulse shapes are hard to implement on shorter time scales, for instance, with femtosecond pulses, because of the prohibitively large Fourier spectrum of a rectangular pulse. Ultrashort pulses hold a great promise for quantum computation because of the absence of decoherence and the emergence of techniques for selective and efficient control of qubits [16, 17]. Such ultrashort pulses can be shaped [18, 19] to have smoothly-varying bell-shaped envelopes, e.g., gaussian or hyperbolic-secant. The theory of composite sequences of pulses with such smooth envelopes, unlike the extensive literature of excitation by single pulses [20–28], is largely missing, which has limited hitherto the use of this powerful control technique on short and ultrashort time scales.

In this paper, we present a simple systematic approach, which allows the construction of composite sequences of pulses with smooth shapes that can create broadband, narrowband and passband excitation profiles corresponding to effective π and fractional-π pulses, with any desired flatness. Our method is based upon the SU(2) representation of the propagator of the two-state system [29], instead of the commonly used intuitive SO(3) rotations in the Bloch vector picture [1–9]. The latter provide geometric depiction of the action of the composite pulse, but are more demanding numerically. The SU(2) approach allows us to use the available exact analytic solutions for special pulse shapes, which in turn allow us to obtain the phases of the respective composite pulses. We will find that up to a certain number of ingredient pulses the composite phases are independent of the pulse shapes.

II. PROPAGATOR OF A COMPOSITE PULSE SEQUENCE

A pure state of a coherently driven two-state quantum system is described, in the interaction representation, by the state vector

$$|\Psi(t)\rangle = \sum_{n=1}^{2} c_n(t)\, \mathrm{e}^{-\mathrm{i}E_n t/\hbar}|n\rangle, \tag{1}$$

where E_n are the eigenenergies of the unperturbed Hamiltonian $\mathbf{H}_0$, $\mathbf{H}_0|n\rangle = E_n|n\rangle$, and $c_n(t)$ is the complex-valued probability amplitude of state $|n\rangle$. The amplitudes $c_1(t)$ and $c_2(t)$ are solutions of the Schrödinger equation,

$$\mathrm{i}\hbar\partial_t \mathbf{c}(t) = \mathbf{H}(t)\mathbf{c}(t), \tag{2}$$

where $\mathbf{H}(t)$ is the Hamiltonian of the system. We will assume that $E_2 \geqq E_1$; then the Bohr transition frequency will be $\omega_0 = (E_2 - E_1)/\hbar$. In the presence of an external coherent field and after performing the rotating-wave approximation (RWA), the Hamiltonian reads

$$\mathbf{H}(t) = \frac{\hbar}{2}\begin{bmatrix} 0 & \Omega(t)\,\mathrm{e}^{-\mathrm{i}D(t)} \\ \Omega(t)^*\,\mathrm{e}^{\mathrm{i}D(t)} & 0 \end{bmatrix}, \tag{3}$$

with $D(t) = \int_{t_i}^{t} \Delta(t')\mathrm{d}t'$, where $\Delta = \omega_0 - \omega$ is the detuning between the laser carrier frequency ω and the Bohr transition frequency ω_0. For electric-dipole transitions the Rabi frequency $\Omega(t)$ parameterizes the coupling between the electric field $\mathbf{E}(t)$ and the transition dipole moment $\mathbf{d}$: $\Omega(t) = -\mathbf{d}\cdot\mathbf{E}(t)/\hbar$; for two-photon Raman

transitions the Rabi frequency is proportional to $\mathbf{E}(t)^2$. The evolution of the system is described by the propagator $\mathbf{U}$, which connects the values of the amplitudes at the initial and final times, t_i and t_f: $\mathbf{c}(t_\mathrm{f}) = \mathbf{U}(t_\mathrm{f}, t_\mathrm{i})\mathbf{c}(t_\mathrm{i})$. The propagator is conveniently parameterized with the complex Cayley-Klein parameters a and b as

$$\mathbf{U} = \begin{bmatrix} a & b \\ -b^* & a^* \end{bmatrix}. \tag{4}$$

For exact resonance ($\Delta = 0$), the Schrödinger equation is solved exactly for any $\Omega(t)$. Then the Cayley-Klein parameters depend only on the pulse area $A = \int_{t_\mathrm{i}}^{t_\mathrm{f}} \Omega(t)\mathrm{d}t$:

$$a = \cos(A/2), \qquad b = -\mathrm{i}\sin(A/2), \tag{5}$$

with $\Omega(t)$ assumed real. The transition probability is $p = |b|^2 = \sin^2(A/2)$ and hence complete population inversion occurs for $A = \pi$ (π-pulses) or odd-integer multiples of π. This inversion is sensitive to variations in the pulse area: a small deviation ϵ from the value π, i.e. $A = \pi(1+\epsilon)$, causes an error in the inversion of order $\mathcal{O}(\epsilon^2)$: $p = 1 - \pi^2\epsilon^2/4 + \mathcal{O}(\epsilon^4)$. This sensitivity to errors can be greatly reduced, to any desired order, by replacing the single π-pulse by a composite pulse sequence.

A constant phase shift ϕ in the Rabi frequency, $\Omega(t) \to \Omega(t)\,\mathrm{e}^{\mathrm{i}\phi}$, is imprinted into the propagator (4) as

$$\mathbf{U}_\phi = \begin{bmatrix} a & b\,\mathrm{e}^{-\mathrm{i}\phi} \\ -b^*\,\mathrm{e}^{\mathrm{i}\phi} & a^* \end{bmatrix}. \tag{6}$$

A sequence of N pulses, each with area A_k and phase ϕ_k, produces the propagator

$$\mathbf{U}^{(N)} = \mathbf{U}_{\phi_N}(A_N)\mathbf{U}_{\phi_{N-1}}(A_{N-1})\cdots\mathbf{U}_{\phi_1}(A_1). \tag{7}$$

Equations (5)-(7) allow us to calculate the propagator produced by a composite sequence of pulses; it depends explicitly on the areas A_k and the phases ϕ_k of the ingredient pulses.

III. COMPOSITE π-PULSES

A. Conditions for the composite phases

Our objective is to produce an excitation profile that is maximally robust to variations in the pulse area A at selected value(s) of A. Contrary to most known composite pulses, we assume for simplicity that all pulse areas are equal, $A_k = A(1+\epsilon)$ ($k = 1, 2, \ldots, N$). This assumption is natural for pulsed lasers because they produce a train of possibly imperfect but identical pulses. It is relatively easy to impose a different phase on each pulse by using an electro-optical modulator or a pulse shaper [18, 19]. We consider an odd number of pulses, $N = 2n+1$, although this assumption is not crucial; the rationale behind this is that for $A = \pi$ and $\epsilon = 0$ the composite pulse sequence has the action of a $(2n+1)\pi$ pulse (apart from a phase shift), that causes a perfect inversion. We also require that the composite sequence is symmetric with respect to reversal of pulses, i.e. the phases obey $\phi_k = \phi_{N+1-k}$; this "anagram" condition leads to symmetric inversion profiles. Because the overall phase of the composite sequence is irrelevant, but only the relative phases of the pulses matter for the population changes, we set $\phi_1 = \phi_N = 0$; hence we have n different phases, which are treated as free parameters.

The next step is to calculate the overall propagator (7), and set the first n non-vanishing derivatives of $U_{11}^{(N)}$ with respect to the pulse area A to zero at the desired value of A. In such a manner we obtain a system of n coupled nonlinear algebraic equations for the n phases. The symmetry assumption about the phases, $\phi_k = \phi_{N+1-k}$, ensures that either all even-order or all odd-order derivatives vanish; hence the n phases allow us to nullify the first $2n$ derivatives.

We use this approach to derive the phases for three major types of composite pulses: broadband (BB), narrowband (NB) and passband (PB) pulses [6–8]. For the BB pulses, we require a flat top of the excitation profile at pulse area $A = \pi$; for the NB pulses, we require a flat bottom at area $A = 0$ (or $A = 2\pi$); for the PB pulses, we require a flat bottom at $A = 0$ and a flat top at $A = \pi$. In brief, the composite phases for all BB, NB and PB sequences presented below are derived from the following conditions:

$$\text{BB}: \quad [\partial_A^k U_{11}^{(N)}]_{A=\pi} = 0 \quad (k = 1, 3, \ldots, N-2); \tag{8a}$$

$$\text{NB}: \quad [\partial_A^k U_{11}^{(N)}]_{A=0} = 0 \quad (k = 2, 4, \ldots, N-1); \tag{8b}$$

$$\begin{aligned}\text{PB}: \quad & [\partial_A^k U_{11}^{(N)}]_{A=\pi} = 0 \quad (k = 1, 3, \ldots, M), \\ & [\partial_A^k U_{11}^{(N)}]_{A=0} = 0 \quad (k = 2, 4, \ldots, N-M-2),\end{aligned} \tag{8c}$$

with $\partial_A^k \equiv \partial^k/\partial A^k$. For each N, there are multiple solutions to these conditions.

B. Broadband composite sequences

We have derived an analytic formula for the phases of a BB pulse composed of an arbitrary number of pulses,

$$\phi_k^{(N)} = \left(N + 1 - 2\left\lfloor\frac{k+1}{2}\right\rfloor\right)\left\lfloor\frac{k}{2}\right\rfloor\frac{\pi}{N}, \tag{9}$$

where $k = 1, 2, \ldots, N$ and the symbol $\lfloor x \rfloor$ denotes the floor function (the integer part of x). Such a pulse nullifies the first $2N-1$ derivatives of the transition probability versus the pulse area at the point $A = \pi$; hence the error ϵ is suppressed to order $\mathcal{O}(\epsilon^{2N})$,

$$p = 1 - (\pi\epsilon/2)^{2N} + \mathcal{O}(\epsilon^{2N+2}). \tag{10}$$

In this manner, an arbitrarily flat inversion profile versus the pulse area can be produced. In Table I we show

N	Phases (in units π/N)
3	0 2 0
5	0 4 2 4 0
7	0 6 4 8 4 6 0
9	0 8 6 12 8 12 6 8 0
11	0 10 8 16 12 18 12 16 8 10 0
13	0 12 10 20 16 24 18 24 16 20 10 12 0
15	0 14 12 24 20 30 24 32 24 30 20 24 12 14 0

TABLE I: Phases of BB composite sequences for different number N of ingredient resonant π pulses.

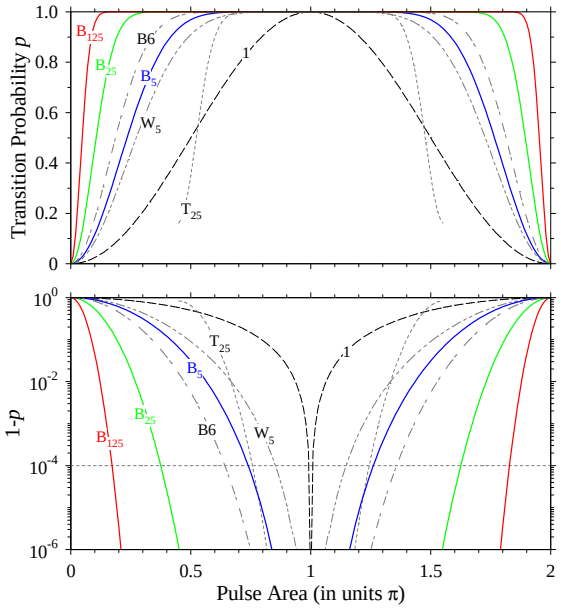

FIG. 1: (Color online) *Top frame:* Transition probabilities p for N-component BB composite sequences B_N versus the area of the ingredient pulses. The composite phases are given by Eq. (9). The dashed curve shows the single π-pulse profile for easy reference. Our composite sequences are compared with other popular composite pulses: W_5 is the BB1 pulse of Wimperis [8], T_{25} is Tycko's 25-pulse sequence [6], and B6 is Brown's 892-pulse sequence [30]. *Bottom frame:* Fidelity of the profiles from the upper frame.

N	Phases (in units π)
5	0; 1.161; 0.580; 1.161; 0
9	0; 1.129; 0.822; 0.108; 1.386; 0.108; 0.822; 1.129; 0
13	0; 0.897; 1.124; 1.846; 0.292; 0.981; 1.771; 0.981; 0.292; 1.846; 1.124; 0.897; 0
17	0; 1.604; 0.553; 1.091; 0.888; 0.620; 1.535; 0.149; 1.569; 0.149; 1.535; 0.620; 0.888; 1.091; 0.553; 1.604; 0

TABLE II: Approximate phases of NB composite sequences for different number N of ingredient resonant π pulses.

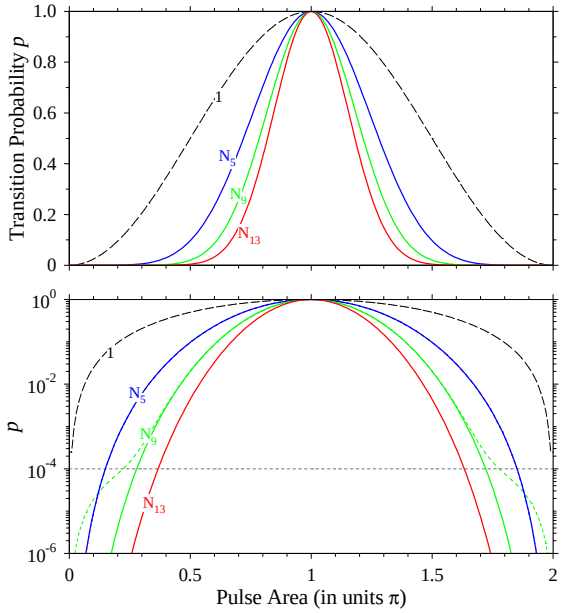

FIG. 2: (Color online) *Top frame:* Transition probabilities p for N-component NB composite sequences N_N versus the area of the ingredient pulses. The composite phases are listed in Table II. The dashed curve shows the single π-pulse profile for easy reference. *Bottom frame:* The transition probabilities from the upper frame on logarithmic scale, which reveals the expansion of the no-transition zones around areas $A = 0$ and 2π as the number of ingredient pulses increases. The dashed curve depicts the transition probability when a random error of 1% is included in the phases of the N_9 pulse.

the explicit phases $\phi_k^{(N)}$ for a few N. For $N = 3$, we find the well-known composite pulse $(\pi)_0(\pi)_{\frac{2}{3}\pi}(\pi)_0$ [2–5]. For $N = 5$, we obtain the composite pulse $(\pi)_0(\pi)_{\frac{4}{5}\pi}(\pi)_{\frac{2}{5}\pi}(\pi)_{\frac{4}{5}\pi}(\pi)_0$, which appears to be new, like all solutions for larger N.

Figure 1 shows the excitation profiles for a few BB pulses with phases from Eq. (9). The profiles can be made arbitrarily flat by increasing the number of pulses, cf. the exotic example with 125 pulses. The logarithmic scale in the bottom frame allows us to examine the fidelity of the profiles against the 10^{-4} benchmark level in quantum information [31]. The range of pulse areas wherein the inversion error remains below 10^{-4} increases dramatically with N: from deviation of 0.006π for a single pulse, to $0.26\pi, 0.62\pi, 0.82\pi$ for $N = 5, 25, 125$, respectively. Our pulses clearly outperform some well-known composite pulses shown in the figure for comparison.

C. Narrowband and passband composite sequences

Figure 2 shows the excitation profiles for a few NB composite sequences and Fig. 3 for a few PB sequences. Unlike BB sequences, we have not been able to find general analytic expressions for the composite phases of NB and PB sequences; the numerical values are given in Tables II and III. For NB sequences the excitation in the wings of the profile is suppressed. PB sequences sup-

N	M	Phases (in units π)
7	1	0; 0.704; 1.186; 1.834; 1.186; 0.704; 0
9	3	0; 0.607; 1.088; 1.472; 0.226; 1.472; 1.088; 0.607; 0
11	1	0; 0.778; 0.609; 1.305; 1.572; 0.137; 1.572; 1.305; 0.609; 0.778; 0
11	5	0; 0.801; 1.144; 1.649; 0.229; 0.944; 0.229; 1.649; 1.144; 0.801; 0
13	3	0; 0.618; 0.210; 1.495; 0.740; 1.288; 1.428; 1.288; 0.740; 1.495; 0.210; 0.618; 0
13	7	0; 0.823; 0.615; 1.243; 1.317; 0.058; 1.925; 0.058; 1.317; 1.243; 0.615; 0.823; 0
15	1	0; 1.146; 0.882; 0.294; 1.822; 1.341; 0.720; 1.950; 0.720; 1.341; 1.822; 0.294; 0.882; 1.146; 0
15	5	0; 0.473; 0.421; 1.624; 1.050; 1.081; 1.469; 0.259; 1.469; 1.081; 1.050; 1.624; 0.421; 0.473; 0
15	9	0; 0.792; 0.681; 1.139; 1.582; 1.778; 0.254; 1.088; 0.254; 1.778; 1.582; 1.139; 0.681; 0.792; 0

TABLE III: Approximate phases of PB composite sequences for different number N of ingredient resonant π pulses. The integer number M indicates the highest derivative annulled at area $A = \pi$, see Eq. (8c), i.e., the larger M the flatter the top of the excitation profile.

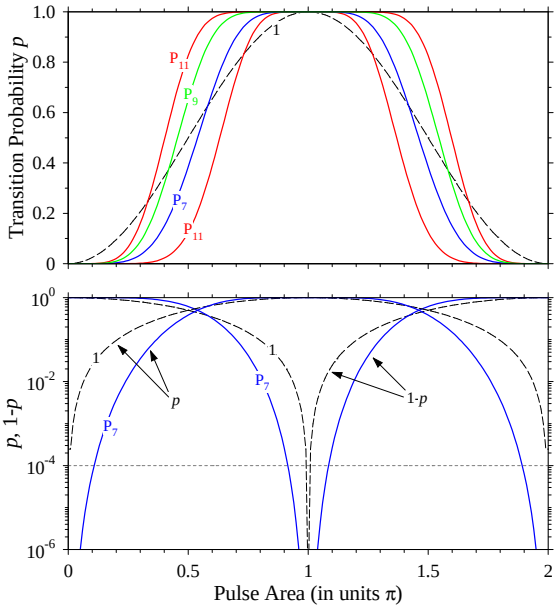

FIG. 3: (Color online) Top frame: Transition probabilities p for N-component PB composite sequences P_N versus the area of the ingredient pulses. The composite phases are listed in Table III. The dashed curve shows the single π-pulse profile for easy reference. *Bottom frame:* Fidelity of the P_7 profile from the upper frame.

press both p in the wings and $1-p$ in the center, i.e., they stabilize the excitation profile at both areas 0 (and 2π) and π. All these features are achieved even for low-N sequences.

In order to examine the sensitivity of the excitation against imperfections in the composite phases, we have included a random noise of 1% in the phases for the N_9 pulse in Fig. 2 (dashed curve in bottom frame). Such an accuracy in the phases is readily achieved with most phase shifting devices. Clearly, a phase noise of this order does not affect the profile dramatically. We have reached similar conclusions for the other excitation profiles as well (not shown for the sake of brevity).

IV. FRACTIONAL-π PULSES

The proposed method for design of composite sequences can be used to construct fractional-π composite sequences, which produce robust coherent superpositions of states. We take a sequence of $N = 2n+1$ pulses with the same area and we determine their phases by fixing the transition probability p to the desired value, $\sin^2\vartheta$, and annulling the first $n-1$ nonzero derivatives at the desired fractional-π value, $A = \vartheta$. For illustration, we consider a half-π composite pulse ($\vartheta = \pi/2$), which produces a coherent superposition with equal probabilities of the two states. The composite phases are determined

N	Phases (in units π)
5	0; 0.765; 0.891; 0.765; 0
7	0; 1.509; 1.029; 0.182; 1.029; 1.509; 0
9	0; 1.319; 1.830; 0.430; 0.794; 0.430; 1.830; 1.319; 0
11	0; 0.509; 0.028; 1.286; 1.258; 0.205; 1.258; 1.286; 0.028; 0.509; 0
13	0; 1.843; 0.452; 1.234; 0.758; 0.528; 1.101; 0.528; 0.758; 1.234; 0.452; 1.843; 0

TABLE IV: Approximate phases of half-π composite sequences for different number N of ingredient resonant $\pi/2$ pulses.

from the following conditions,

$$[U_{11}^{(N)}]_{A=\pi/2} = 1/\sqrt{2}, \tag{11a}$$

$$[\partial_A^k U_{11}^{(N)}]_{A=\pi/2} = 0 \quad (k = 1, 2, \ldots, n-1). \tag{11b}$$

Table IV lists a few sets of phases for difference composite sequences. Figure 4 shows the excitation profiles for several half-π composite sequences, which produce transition probability $p = \frac{1}{2}$ at and around the value $A = \pi/2$. The stabilization of the transition probability around the value $p = \frac{1}{2}$ is similar to the one around the value $p = 1$ for BB composite π pulses in Fig. 1 and to the stabilization around the value $p = 0$ for NB composite sequences in Fig. 2.

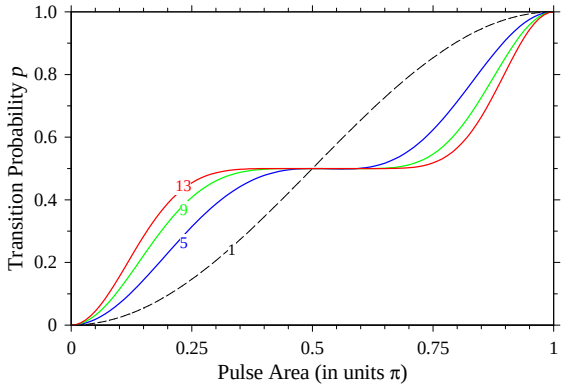

FIG. 4: (Color online) Transition probabilities p for N-component half-π composite sequences versus the area of the ingredient pulses. The area of each ingredient pulse is $\pi/2$ and the composite phases are listed in Table IV.

V. DETUNING-COMPENSATED COMPOSITE SEQUENCES

Up to now, we showed that our resonant composite sequences can produce arbitrarily flat excitation profiles versus the pulse area at various probabilities. We now show that the same SU(2) method can be used to stabilize the excitation profiles with respect to the frequency detuning around exact resonance. Because for nonzero detuning the Cayley-Klein SU(2) parameters depend on the pulse shape of the driving field, one might expect that the composite phases will depend on the pulse shape too. Moreover, one expects that the explicit form of the Cayley-Klein parameters is needed for the derivation of the composite phases, as for resonant pulses. Therefore we begin with an analytically exactly soluble model, with a hyperbolic-secant pulse shape, and then we show that under some symmetry conditions, the composite phases do not depend on the pulse shape up to a certain order.

A. Hyperbolic-secant pulse shape

In the famous Rosen-Zener model [20], the pulse has a hyperbolic-secant shape and a constant detuning,

$$\Omega(t) = \Omega_0 \operatorname{sech}(t/T), \quad \Delta(t) = \text{const.} \tag{12}$$

For this model the Cayley-Klein parameters are [20]

$$a = \frac{\Gamma\left(\frac{1}{2} + \mathrm{i}\delta\right)^2}{\Gamma\left(\frac{1}{2} + \mathrm{i}\delta - \alpha\right)\Gamma\left(\frac{1}{2} + \mathrm{i}\delta + \alpha\right)}, \tag{13a}$$

$$b = -\mathrm{i}\frac{\sin\pi\alpha}{\cosh\pi\delta}, \tag{13b}$$

with $\alpha = \Omega_0 T/2$ and $\delta = \Delta T/2$. The transition probability is $p = |b|^2 = \sin^2\pi\alpha \operatorname{sech}^2\pi\delta$, which means that complete population inversion takes place for $\Omega_0 T = (2k+1)$ (with k integer) and $\Delta = 0$. We take again

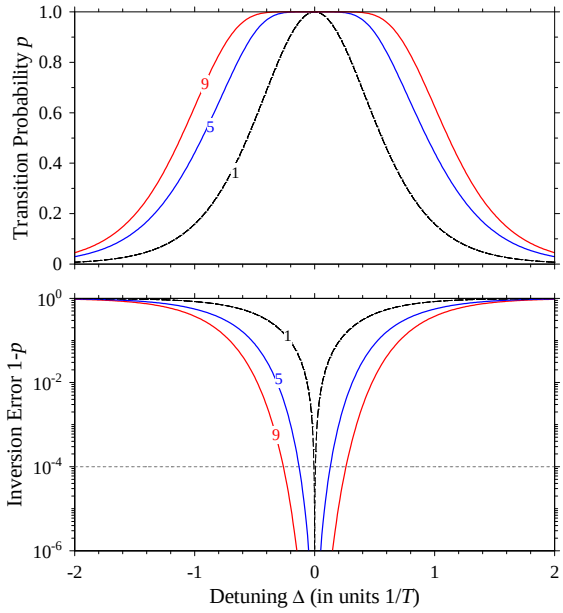

FIG. 5: (Color online) Transition probability p (top) and the error $1-p$ (bottom) versus the detuning for a single sech pulse and for a sequence of five $3\pi/5$ pulses with phases (approximately) $(0, 0.747, 0.424, 0.747, 0)\pi$, and nine $4\pi/9$ pulses with phases $(0, 1.308, 1.153, 1.251, 0.562, 1.251, 1.153, 1.308, 0)\pi$.

$N = 2n+1$ pulses with the same area and symmetric phases, $\phi_{N+1-k} = \phi_k$ $(k = 1, 2, \ldots, n)$, so that the excitation profile is symmetric versus Δ. We multiply the SU(2) propagators for each ingredient pulse and then we set the first $n-1$ derivatives of $U_{11}^{(N)}(\Delta)$ with respect to Δ to zero at $\Delta = 0$,

$$[\partial_\Delta^k U_{11}^{(N)}]_{\Delta=0} = 0 \quad (k = 0, 1, \ldots, n-1). \tag{14}$$

We determine the composite phases from the resulting set of algebraic equations. In general, there are multiple solutions for each N. For $N = 3$, a Δ-compensated pulse is $\pi_0\pi_{\pi/3}\pi_0$. For larger N, the phases are derived numerically. Figure 5 shows the excitation profiles for a few Δ-compensated composite sequences. As the lower frame shows, even moderately large composite sequences greatly enhance the 10^{-4} error tolerance range: from detunings $\pm 0.006/T$ for a single pulse to $\pm 0.13/T$ for the five-pulse sequence and $\pm 0.26/T$ for the nine-pulse sequence.

B. General case

The described method, although well suited for analytically soluble models, can be applied to arbitrary pulse shapes too, e.g. gaussian, $\Omega(t) = \Omega_0 \mathrm{e}^{-t^2/T^2}$. We have found that the phases of composite sequences of up to five pulses do not depend on the pulse shape provided the latter is symmetric,

$$\Omega(-t) = \Omega(t). \tag{15}$$

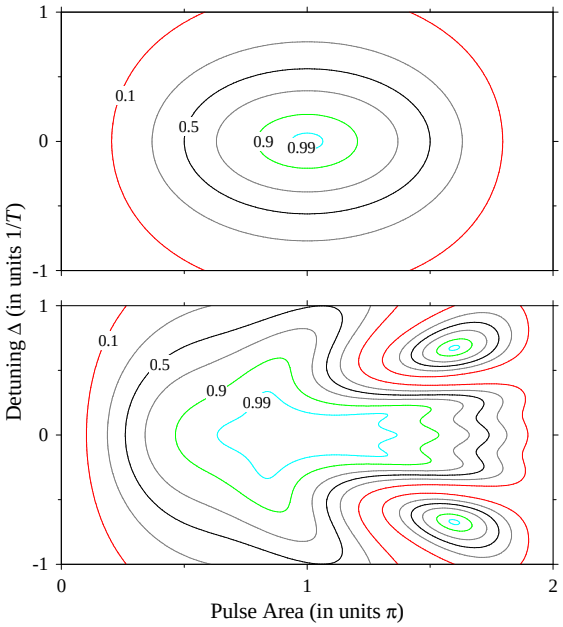

FIG. 6: (Color online) Transition probability versus detuning and pulse area for a single pulse (upper frame) and for a five-pulse composite sequence with phases $(0, 5\pi/6, \pi/3, 5\pi/6, 0)$ (lower frame).

In order to prove this we use the fact that for such pulse shapes the Cayley-Klein parameters can be written as

$$a = f_{\rm e}(\Delta) + {\rm i} f_{\rm o}(\Delta), \quad b = -{\rm i}\sqrt{1 - f_{\rm e}^2(\Delta) - f_{\rm o}^2(\Delta)}, \tag{16}$$

where the labels 'e' and 'o' stand for even and odd functions, respectively. We also note that after differentiation, an odd function becomes even and vice versa. Next, we obtain the Taylor expansion of a at $\Delta = 0$ and set the first few terms to zero (the more phases we have, the more terms we can nullify). Then we notice that, due to Eq. (16), the equations for the phases do not depend on the particular forms of $f_{\rm e}$ and $f_{\rm o}$. This property is conserved for sequences of up to five pulses, which means that the respective composite phases are universal.

C. Simultaneous stabilization versus pulse area and detuning

Another application of this method is for obtaining profiles that are flat versus both A and Δ. The phases are derived in the same way as before, but now we nullify derivatives versus both A and Δ,

$$\left[\frac{\partial^{k_1+k_2}}{\partial A^{k_1}\partial\Delta^{k_2}}\right]_{(A=\pi,\Delta=0)} = 0, \tag{17}$$

where the values of k_1 and k_2 determine the flatness versus the respective parameter A and Δ. An example for a five-pulse composite sequence is shown in Fig. 6. It demonstrates how the small high-fidelity central spot in the upper frame is greatly expanded by the composite sequence in the lower frame.

VI. DISCUSSION

A. Pulse sequences

The composite pulse sequences presented in this paper can be produced in various manners. Pulsed laser systems operating at repetition rates 100 MHz, in combination with standard programmable phase shifters, can produce composite sequences of pulses with time duration on the scale of 100 ns. One can, however, use a femtosecond pulse shaper in order to produce composite sequences on femtosecond time scale. For example, consider a sequence of $2n+1$ $\cos^{2s}$-pulses (with s a positive integer), with the following Rabi frequency in the time domain

$$\Omega(t) = \begin{cases} \cos^{2s}(t/T), & -(n+\frac{1}{2})\pi T \leqq t \leqq (n+\frac{1}{2})\pi T, \\ 0, & \text{otherwise.} \end{cases} \tag{18}$$

Let us impose on each pulse a phase as given by Eq. (9) and explicitly shown in Table I. In order to produce this model by femtosecond pulse shaping technology, one needs to know the Fourier spectrum of the pulse sequence, which is readily computed; however, it is too long to be shown here. What is very important is that the Fourier spectra of our composite sequences, with the pulse shapes of Eq. (18) and the phases of Eq. (9), have the following asymptotic behavior at large frequencies, regardless of the number of ingredient pulses:

$$\widetilde{\Omega}(\omega) \sim \mathcal{O}(\omega^{-2s-1}). \tag{19}$$

This rapid decrease makes femtosecond pulse shaping, and coherent control by composite sequences on femtosecond time scale, possible.

We note here that the composite sequences derived by us require pulse areas of π (or less) for the ingredient pulses. Excitation with such pulse areas has already been achieved in femtosecond physics; it has been shown that pulses with well controlled areas of several π [32–34], and even adiabatic evolution which requires larger pulse areas [35–37], can be achieved.

B. Decoherence

The composite sequences derived in this paper did not take decoherence into account. This assumption is reasonable in various implementations. As explained above, our technique is applicable to the femtosecond time scale when the pulse sequence is produced by a pulse shaper; then decoherence is largely irrelevant. On the longer time scales, decoherence should be taken into account if one of the qubit states is an excited electronic state. However,

in quantum information processing, the qubit is usually composed of two ground states, or a ground state and a metastable state, connected with a two-photon Raman transition. Then a coherence time larger than 1 second can be achieved [10–15], and decoherence can be ignored. We note here that decoherence can be suppressed with approaches similar to composite pulse sequences, known as "dynamical suppression of decoherence" [38].

C. Phase jitter

Because the technique of composite sequences demands relatively accurately specified relative phases of the ingredient pulses, the control over these phases is the most important part of the technique. It is therefore essential to know and control the possible sources of phase jitter. In Fig. 2 (lower frame) we have included a (dashed-curve) excitation profile, in which a random phase jitter of 1% was introduced. Phase shifts with an uncertainty well below this value are readily obtained with standard pulse shapers (for femtosecond pulses) and phase shifters (for nanosecond and microsecond pulses).

A more important issue to address is the free evolution phase shift between the two states of the qubit, which interferes with the composite phases; such a phase should be incorporated in the composite phases. We note that because we work in the interaction representation, Eq. (1), and in RWA, it is the frequency detuning that determines the free-evolution phase, rather than the transition frequency. On resonance such a phase shift is naturally absent. For off-resonant pulses, this phase should be accounted for in the calculation of the phases.

VII. CONCLUSION

We presented a general method for design of a huge variety of composite sequences of pulses with smooth temporal shapes. This allows the application of composite sequences to coherent atomic excitation with short and ultrashort laser pulses. Because our method uses SU(2) propagators in the Schrödinger picture instead of the commonly used SO(3) rotations in the Bloch picture, it is simpler both algebraically and numerically and easily generates many new solutions, which appear superior to the known ones, cf. Fig. 1. An important advantage of our method is that the resulting composite pulses produce excitation profiles in which the robustness against variations in the parameters is accompanied with ultrahigh fidelity, well beyond the fault tolerance limit of quantum computation [31]; this is a topic, which is rarely, if ever, investigated in the literature on composite pulses. We have found that composite pulse sequences are ideally suited for this objective. On resonance ($\Delta = 0$), the composite sequences do not depend on the pulse shape; our method has allowed us to derive a variety of broadband, narrowband and passband sequences of arbitrary flatness with regard to the pulse area. In particular, we have found a simple analytic formula for the phases of arbitrary accurate broadband sequences. It is particularly important that this independence on the pulse shape is extended also off resonance, for composite sequences composed of up to five identical single pulses. This universality is of potential significance in cases when the desired pulse shape is hard to produce. We also point out that, because smooth temporal shapes induce exponential dependence of the excitation probability on Δ [20, 39], such pulse shapes facilitate the elimination of sidebands in the excitation profiles of Δ-compensated composite pulses, which are always present with rectangular pulse shapes. This suppression of excitation sidebands is of potential significance for selective manipulation of collective states of many-particle systems in quantum information processing.

Acknowledgments

This work is supported by the European Commission project FASTQUAST and the Bulgarian NSF grants VU-I-301/07, D002-90/08 and DMU02-19/09.

[1] E. L. Hahn, Phys. Rev. **80**, 580 (1950).
[2] M. H. Levitt and R. Freeman, J. Magn. Reson. **33**, 473 (1979).
[3] R. Freeman, S. P. Kempsell, and M. H. Levitt, J. Magn. Reson. **38**, 453 (1980).
[4] M. H. Levitt, Prog. NMR Spectrosc. **18**, 61 (1986).
[5] R. Freeman, *Spin Choreography* (Spektrum, Oxford, 1997).
[6] R. Tycko, Phys. Rev. Lett. **51**, 775 (1983); R. Tycko, A. Pines, and J. Guckenheimer, J. Chem. Phys. **83**, 2775 (1985).
[7] H. M. Cho, R. Tycko, A. Pines, and J. Guckenheimer, Phys. Rev. Lett. **56**, 1905 (1986).
[8] S. Wimperis, J. Magn. Reson. **109**, 221 (1994).
[9] H. K. Cummins, G. Llewellyn and J. A. Jones, Phys. Rev. A **67**, 042308 (2003).
[10] S. Gulde, M. Riebe, G. P. T. Lancaster, C. Becher, J. Eschner, H. Häffner, F. Schmidt-Kaler, I. L. Chuang and R. Blatt, Nature **421**, 48 (2003).
[11] F. Schmidt-Kaler, H. Häffner, M. Riebe, S. Gulde, G. P. T. Lancaster, T. Deuschle, C. Becher, C. F. Roos, J. Eschner, and R. Blatt, Nature **422**, 408 (2003).
[12] M. Riebe, H. Häffner, C. F. Roos, W. Hänsel, J. Benhelm, G. P. T. Lancaster, T. W. Körber, C. Becher, F. Schmidt-Kaler, D. F. V. James, and R. Blatt, Nature **429**, 734 (2004).
[13] M. D. Barrett, J. Chiaverini, T. Schaetz, J. Britton, W. M. Itano, J. D. Jost, E. Knill, C. Langer, D. Leibfried,

R. Ozeri, and D. J. Wineland, Nature **429**, 737 (2004).
[14] H. Häffner, C. F. Roos, and R. Blatt, Phys. Rep. **469**, 155 (2008).
[15] N. Timoney, V. Elman, S. Glaser, C. Weiss, M. Johanning, W. Neuhauser, and C. Wunderlich, Phys. Rev. A **77**, 052334 (2008).
[16] D. Hayes, D. N. Matsukevich, P. Maunz, D. Hucul, Q. Quraishi, S. Olmschenk, W. Campbell, J. Mizrahi, C. Senko, and C. Monroe, Phys. Rev. Lett. **104**, 140501 (2010).
[17] W. C. Campbell, J. Mizrahi, Q. Quraishi, C. Senko, D. Hayes, D. Hucul, D. N. Matsukevich, P. Maunz, and C. Monroe, Phys. Rev. Lett. **105**, 090502 (2010).
[18] M. Wollenhaupt, V. Engel, and T. Baumert, Annu. Rev. Phys. Chem. **56**, 25 (2005).
[19] M. Wollenhaupt, A. Assion, and T. Baumert, in *Springer Handbook of Lasers and Optics*, edited by F. Träger (Springer, New York, 2007), Chap. 12.
[20] N. Rosen and C. Zener, Phys. Rev. **40**, 502 (1932).
[21] Yu. N. Demkov and M. Kunike, Vestn. Leningr. Univ. Fiz. Khim. **16**, 39 (1969).
[22] F. T. Hioe and C. E. Carroll, Phys. Rev. A **32**, 1541 (1985).
[23] J. Zakrzewski, Phys. Rev. A **32**, 3748 (1985).
[24] K-A. Suominen, B. M. Garraway, Phys. Rev. A **45**, 374 (1992).
[25] A. E. Kaplan, Sov. Phys. JETP **41**, 409 (1975).
[26] A. E. Kaplan, Sov. J. of Quantum Electronics **6**, 728 (1976).
[27] V. Y. Finkelstein, Sov. Phys. JETP **76**, 91 (1979).
[28] S. P. Goreslavsky and V. P. Krainov, Sov. Phys. JETP **76**, 26 (1979).
[29] N. V. Vitanov and P. L. Knight, Phys. Rev. A **52**, 2245 (1995).
[30] K. R. Brown, A. W. Harrow, and I. L. Chuang, Phys. Rev. A **70**, 052318 (2004).
[31] M. A. Nielsen and I. L. Chuang, *Quantum Computation and Quantum Information* (Cambridge University Press, UK, 2000).
[32] M. Wollenhaupt, A. Assion, O. Bazhan, Ch. Horn, D. Liese, Ch. Sarpe-Tudoran, M. Winter, and T. Baumert, Phys. Rev. A **68**, 015401 (2003).
[33] M. Wollenhaupt, A. Präkelt, C. Sarpe-Tudoran, D. Liese, T. Bayer, and T. Baumert, Phys. Rev. A **73**, 063409 (2006).
[34] T. Bayer, M. Wollenhaupt, C. Sarpe-Tudoran, and T. Baumert, Phys. Rev. Lett. **102**, 023004 (2009).
[35] M. Wollenhaupt, A. Präkelt, C. Sarpe-Tudoran, D. Liese, and T. Baumert, Appl. Phys. B **82**, 183 (2006).
[36] B. D. Bruner, H. Suchowski, N. V. Vitanov, and Y. Silberberg, Phys. Rev. A **81**, 063410 (2010).
[37] M. Krug, T. Bayer, M. Wollenhaupt, C. Sarpe-Tudoran, T. Baumert, S. S. Ivanov, and N. V. Vitanov, New J. Phys. **11**, 105051 (2009).
[38] G. S. Uhrig, Phys. Rev. Lett. **98**, 100504 (2007).
[39] J. P. Davis and P. Pechukas, J. Chem. Phys. **64**, 3129 (1976).